Casting a Healthier Future:

Electrochemical and Microstructural Characterization of the Cu-Zn-Al-Sn Alloy System for Antimicrobial Use

2025-2026

Table of Contents

Abstract 1

Introduction.....2

Hypothesis.....3

Materials and Methods 4

Metal Casting 4

Lost Foam Casting 4

Graphite Mold Casting 5

Risk and Safety 5

Electrochemical Testing 6

Working Electrode Preparation 6

Open Circuit Potential Experiments 7

Potentiostatic Electrochemical Impedance Spectroscopy (PEIS) 7

Antimicrobial Testing 8

Chemical and Microstructural Characterization 9

X-Ray Fluorescence Spectroscopy (XRF) 9

Scanning Electron Microscopy (SEM) 9

Results and Discussion 10

Metal Casting Results 10

Electrochemical Characterization 12

Impedance Data (PEIS) 13

Antimicrobial Assay Results 15

SEM BSED Analysis 17

Conclusions 19

Observed Trends 19

Winning Alloy Candidates 19

Works Cited 20

Abstract

Copper is a widely used and studied antimicrobial agent that has been proposed and implemented in healthcare settings to reduce bacterial spread. Issues arising from the longevity and cost of copper as a surface coating present significant roadblocks to widespread implementation. Introducing alloying elements could fine-tune desired properties while simultaneously maintaining a lower cost. Different compositions of alloys can affect the antimicrobial and corrosion-resistant properties of copper alloys.

This study investigates the Cu-Zn-Al-Sn alloy system in the copper-rich corner, with tin held near 1% of the alloy composition. The research aims to determine whether described antimicrobial results can be achieved with alloying elements simultaneously enhancing corrosion resistance and reducing material cost. Past studies suggest that copper and zinc contribute to the majority of the antimicrobial effort due to their mechanisms of attack, which disrupt respiratory chains, metabolism, and oxide regulatory chains, all of which severely impact bacterial survival (Horton et al., 2015; David, 2011).

Chemical analysis of alloy composition was performed using X-ray Fluorescence Spectroscopy (XRF) and partially with Energy Dispersive Spectroscopy (BSED). Electrochemical analysis was conducted using Open Circuit Potential (OCP) and Potentiostatic Electrochemical Impedance Spectroscopy (PEIS). Antimicrobial testing was performed using a modified ISO 22196 protocol with a contact time of two hours, followed by recovery and assay. Results demonstrated that Alloys 1, 3, and 7 achieved a >5-log reduction (99.999% kill) of E. coli within 120 minutes, with Alloy 1 demonstrating a statistically significant ($p < 0.05$) increase in corrosion resistance (R_{xt} = 404.61 $\Omega \cdot cm^2$). At approximately 15 minutes, a significant statistical test of log reduction combined with compositional differences of alloy 1 and 3 suggest copper content still continuing to be the main driver of bacterial efficacy.

Introduction

The motivation behind conducting this set of experiments is to further discover the application potential of different metals for commercial use. Many metals exist for architectural applications, such as stainless steel, brass, and aluminum. However, many of these metals are used without considering the lack of microbial protection they provide. Experimenting with varying ratios of the Cu-Zn-Al-Sn alloy system is valuable in seeking a replacement for architectural features such as railings or handles to better prevent the spread of disease.

In the United States, the Environmental Protection Agency (EPA) is the governing institution for determining the use of copper and copper alloys for antimicrobial applications. It is important to emphasize that the use of these metals should not replace existing sanitation practices but should serve as an additional layer of protection. The lowest copper percentage approved by the EPA for antimicrobial purposes is 60-64.05%, tested to inhibit 99.99% of bacteria with a 2-hour contact time (Khan et al., 2022).

Another important consideration when designing antimicrobial alloys is their potential use for marine applications. Existing paint mixtures use pure copper or copper oxide powder to prevent biofilms from forming on ship hulls. With the addition of aluminum and zinc, it might be possible to create a lighter powder that is equally effective in terms of corrosion and antimicrobial properties. If lighter elements are used, shipping can become more sustainable and cost-effective due to reduced vessel weight, resulting in lower fuel consumption per trip and potentially less time in dry docks for repainting with better corrosion resistance.

When examining an alloy system, four elements—Cu, Zn, Al, and Sn—come to mind for engineering a platform capable of accomplishing the aforementioned tasks. The most researched alloy of this family, Nordic gold (an aluminum brass), possesses unique properties compared to other copper alloys. The alloy is antimycotic, antimicrobial, and exhibits excellent corrosion resistance. Abrasion of the metal enhances the antimicrobial properties further (Foster, 2014). The mechanism for its antimicrobial activity after abrasion occurs due to a thin oxide layer capable of producing Cu^{2+} and Zn^{2+} ions, which detrimentally affect bacterial survival.

Hypothesis and Research question

Researchable Question -

Hypothesis - Increasing the zinc and aluminum ratios of a Nordic Gold baseline will improve corrosion resistance and lower costs, while maintaining 60% will, maintain antimicrobial efficacy.

Materials and Methods

Metal Casting

Alloys were melted and cast at the student researcher's household. Copper, zinc, and tin were purchased from Rotometals.com. Aluminum was sourced from recycled aluminum cans that had been previously melted. The home foundry setup included an argon tank, argon regulator, and electric furnace.

Metals were added in the following order: copper, tin, aluminum, and zinc. Casting was performed using two methods. All metal casting procedures were conducted outside and at night. A nearby bucket of sand was present to extinguish any possible fires.

Lost Foam Casting

Alloys 1, 2, 3, 6, 7, and 9 were produced using a lost foam casting method (labels were not assigned according to casting order). Styrofoam 2.1 cm (1 inch) rods were coated with refractory cement to form molds, which were subsequently placed in petrobond (oil-bonded) sand prior to burnout. Burnout was achieved either by direct flame or by molten metal during pouring. The molten alloy was then poured into the prepared molds and allowed to cool to room temperature. Alloy 6 was excluded from further testing due to excessive porosity observed after solidification.

Graphite Mold Casting

Alloys 4, 5, and 8 were cast using a graphite ingot mold. The mold was preheated to above 230°C and then cooled to remove residual moisture before use. Molten alloy was poured into the prepared mold and allowed to cool to room temperature prior to removal.

Risk and Safety

Given the hazardous nature of metal casting operations, comprehensive safety protocols were implemented throughout all casting procedures:

0. Personal Protective Equipment (PPE) :Flame-resistant lab coat, welding gloves, and full-face carbon filter respirator to protect against zinc fume inhalation.

1. Fire Safety: A bucket of sand was maintained nearby for immediate fire suppression if needed.

Note: Zinc vaporization at temperatures above 1000°C presents significant inhalation hazards. The carbon filter respirator was specifically selected to filter zinc oxide fumes, which can cause metal fume fever if inhaled.

Electrochemical Testing

The potentiostat used was Biologic's SP-200. Electrodes consisted of student-made alloy working electrodes, laboratory-provided $Ag/AgNO_3$ pseudo-reference electrodes, and student-purchased Mixed Metal Oxide (MMO) counter electrodes. Open Circuit Potential (OCP) was measured before Electrochemical Impedance Spectroscopy (EIS). Electrodes were washed with acetone and air-dried before and after each test. Data were collected using Biologic EC-Lab Software, then exported and normalized in Excel with geometric surface area calculated using ImageJ. The test solution was 50 mL artificial sweat solution consisting of 5 g/L NaCl, 1 g/L urea, and 1 g/L lactic acid per replicate.

Working Electrode Preparation

Alloy chips were cut using an angle grinder and sanded flat with P80 SiC paper. A copper wire was soldered to the opposite face to provide electrical contact. Each sample was mounted by placing the flat face on tape and surrounding it with a mold containing a hole to accommodate the wire. Epoxy resin was poured into the mold and cured for 24 hours. The exposed alloy surface was then polished to P1500 grit to serve as the active electrode face.

Open Circuit Potential Experiments

Initial open-circuit potential (OCP) scans were conducted for 15 minutes for all alloys, except for Alloy 7, which was monitored for one hour to confirm equilibrium behavior. Subsequent trials were shortened once OCP values stabilized, indicating the system had reached equilibrium. The extended monitoring for Alloy 7 was chosen following visual inspection of OCP time data from a previous study on approximately the same alloy composition.

Potentiostatic Electrochemical Impedance Spectroscopy (PEIS)

Immediately after each OCP measurement, potentiostatic electrochemical impedance spectroscopy (PEIS) was performed using the following parameters: frequency range of 10^6

to 10^{-3} Hz, sinusoidal perturbation amplitude of 10 mV, and voltage window of -10 V to +10 V.

Antimicrobial Testing

Alloys were tested using a modified version of ISO 22196:2011. Copper alloy antimicrobial properties are tested by inoculating them with bacteria, incubating for a specified contact time, then washing and plating the surviving bacteria. An experimentally determined approximation of ~3.5×10^7 colony-forming units (CFU) original solution was made after serial plating. 30 µL of a 1:10 dilution with phosphate buffer solution was plated onto alloys. Sterile film of 2.1 cm (1 inch) was placed over the inoculum, spread with tweezers, and incubated at 37°C for the specified contact time. After incubation, each alloy was rinsed in 5 mL of neutralizing buffer within sterile bags for 2 minutes to recover attached cells. 100 µL from the bag was then plated onto agar dishes and allowed to incubate at 37°C for 24 hours. Plates were then visually analyzed for qualitative assessment of antimicrobial efficacy.

Chemical and Microstructural Characterization

X-Ray Fluorescence Spectroscopy (XRF)

Elemental alloy composition was determined using an Olympus Delta 2000 XRF Analyzer. Alloys were placed under a dedicated X-ray emitter for 5 minutes per analysis.

Scanning Electron Microscopy (SEM)

Select alloys were analyzed using an FEI Inspec-S Scanning Electron Microscope. Alloy chips were prepared by sanding two faces flat, with one face being sanded with P1500 grit SiC sandpaper. Samples were then placed on double-stick carbon tape and put under vacuum within the SEM. Alloys 3, 4, 5, and 7 were documented. Analysis and backscattered electron imaging of selected sites to document grain homogeneity and potential sub grain features.

Results and Discussion

Metal Casting Results

Alloys 4, 5, and 8 were cast using a graphite ingot mold, while the remaining alloys were cast through lost foam casting. The furnace setup achieved temperatures above 1000°C.

Copper loss was minimal due to the argon blanket and copper's more noble elemental status when compared to zinc and tin. Zinc loss can be attributed to vaporization, as these alloys were melted at 1000°C or higher, which is well above zinc's vaporization point (907°C). Aluminum loss can be attributed to the creation of aluminum dross from oxidation when the furnace was opened to input zinc and tin, as well as the fact that the aluminum source was approximately 97% pure when XRF-analyzed among the metals. Alloy 8 had a major impurity of iron due to a purchased used crucible that was improperly labeled as graphite crucible but was a black painted ceramic crucible . Aside from the iron in Alloy 8, the two major impurities in each alloy were magnesium and silicon, which all came from the recycled aluminum source.

Notable physical properties were observed in several alloys. Alloys 4 and 8 exhibited a dull gray appearance with small porosity visible after abrasion. This porosity could be explained by the precipitation of hydrogen gas, which dissolves in molten aluminum (Tiryakioğlu, 2012).

Table 1 and 2: Target vs. Actual Alloy Compositions (wt%) via XRF Analysis

Target Composition

Name	Cu%	Zn%	Al%	Sn%
Pure Copper	100			
Alloy 1	69	20	10	1
Alloy 2	79	7.5	7.5	1
Alloy 3	79	10	10	1
Alloy 4	69	15	15	1
Alloy 5	69	25	5	1
Alloy 7	89	5	5	1
Alloy 8	79	5	15	1

Actual Composition Sourced Via XRF

Name	Cu%	Zn%	Al%	Sn%	% Impurity
Pure Copper	1				
Alloy 1	68.72	19.44	8.42	1.53	1.89
Alloy 2	83.84	5.46	9.2	1.27	0.23
Alloy 3	78.99	8.94	9.72	1.54	0.81
Alloy 4	68.46	12.69	11.95	1.265	5.635
Alloy 5	69.2	25.1	4.2	1.17	0.33
Alloy 7	87.18	5.72	4.91	1.3	0.89
Alloy 8	79.86	4.97	12.16	1.47	1.54

Figures 1-2: *Target compositions versus measured XRF values. Discrepancies explained by zinc vaporization, aluminum dross formation, and iron impurity from crucible (Alloy 8). (Source: Student-generated data, 2025)*

Electrochemical Characterization

Open Circuit Potential (OCP) Results

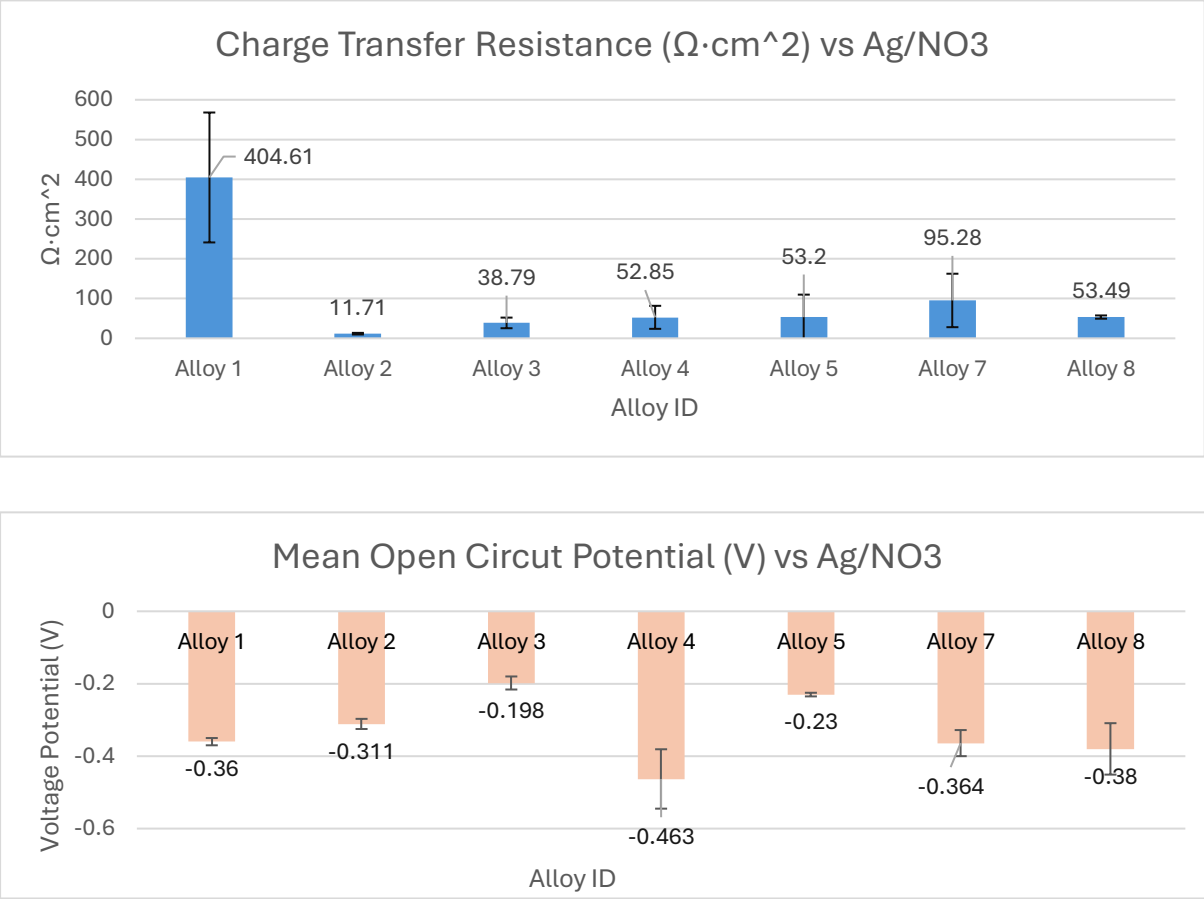

Figure 3-4: Top: Charge Transfer Resistance Rct values.. Bottom: Mean Open Circuit Potential (OCV) vs. Ag/NO3 Values ranged from -0.198 V$ (Alloy 3) to -0.463 V (Alloy 4). Significance testing (p-values) was not performed for OCV data. Note: Error bars indicate standard deviation. (Source: Student-generated data, 2026)

The OCP measurements provide quantitative information on the chemical reactivity of each alloy before corrosion testing begins. Higher (more positive) OCP values indicate more noble (less reactive) metals. The shortest time reference of each replicate alloy was used as the reference axis, with all replicates having undergone an initial OCP test of 15 minutes except Alloy 7, which was monitored for 1 hour.

Higher aluminum content in Alloys 8, 4, 2, and 1 could explain why they are considered more active alloys. Aluminum is the least noble of all the metals with a standard potential of -1.66 V (vs. Standard Hydrogen Electrode), and although it has a stable oxide layer, the other alloying elements do not allow for a stable aluminum oxide layer to form (Šulčius, 2010).

This trend, however, is not observed with Alloy 3, which could indicate that intermetallic phases of α and β brass between the alloying elements zinc and aluminum for copper are more important factor. Alloy 7 remains an outlier within this trend of more aluminum equating more noble metals.

Key Finding: Alloy 3 demonstrated the most noble (least chemically reactive) OCP values, suggesting it would be best suited for applications requiring minimal surface reactivity, such as marine environments where dezincification is a concern.

Impedance Data (PEIS)

Data were graphed with the mean of three replicates that had their impedance components normalized with surface area (Alloy 7 only has 2 replicates due to an instrumentation error). Alloys were fitted with R1+Q2/R2 equivalent Randles Circuit.

Although OCP data provides insight into the chemical activity of the alloy, the impedance collected is a more definitive way to measure corrosion resistance by providing the actual kinetics. The impedance data show that Alloy 5 is oddly the least corrosion-resistant of all the metals. This could be explained by a process known as dezincification, where the chlorides in solution selectively leach out zinc.

Alloy 1 shows the greatest impedance, implying that it is the most corrosion-resistant. The large difference is supported by one replicate in the testing that was nearly double that of the other two. Even with this nuance stated, Alloy 1 still proved statstically significant corrosion resistance. Alloy 1's high zinc ratio to aluminum (but not as high as in Alloy 5) could be the reason for such high impedance.

Alloy 8 shows 4 presented artifacts within the Nyquist and Bode plots, indicating that impurities are causing many more electrochemical processes than the other alloys. Alloy 4 shows a similar result to Alloy 8, implying that intermetallic compounds like the confirmed γ brass seen in both or different oxide layers forming from higher aluminum content can create these overlapping time constants. This claim can be further backed up in XRD analysis where it was discovered that these alloys had gamma ß- brass phases which are known to be less noble then α-brass phases.

Alloy 2's low impedance could also be attributed to a low zinc-to-aluminum ratio, as previously discussed in the OCP data, which suggests not only that it is more chemically

reactive but that the aluminum in this alloy may be forming more aluminum intermetallic, though XRD characterizing would be needed to validate this claim.

Alloy 3 nobleness attributed in OCP measurements, which suggests that it might be the best choice for corrosion-resistant applications in environments that are extremely harsh.

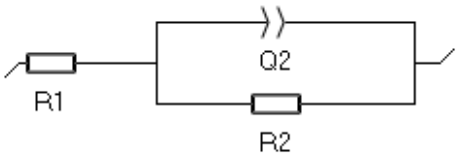

Figure 5: Randles Equivalent Circuit Model. *A representative Randles equivalent circuit (R+1(Q2/R2)) was used for fitting experimental data, where R1 represents solution resistance and the Q2/R2 parallel combination models the capacitive and charge transfer characteristics of the alloy-electrolyte interface.). (Source: EC-Circuit lab)*

Antimicrobial Assay Results

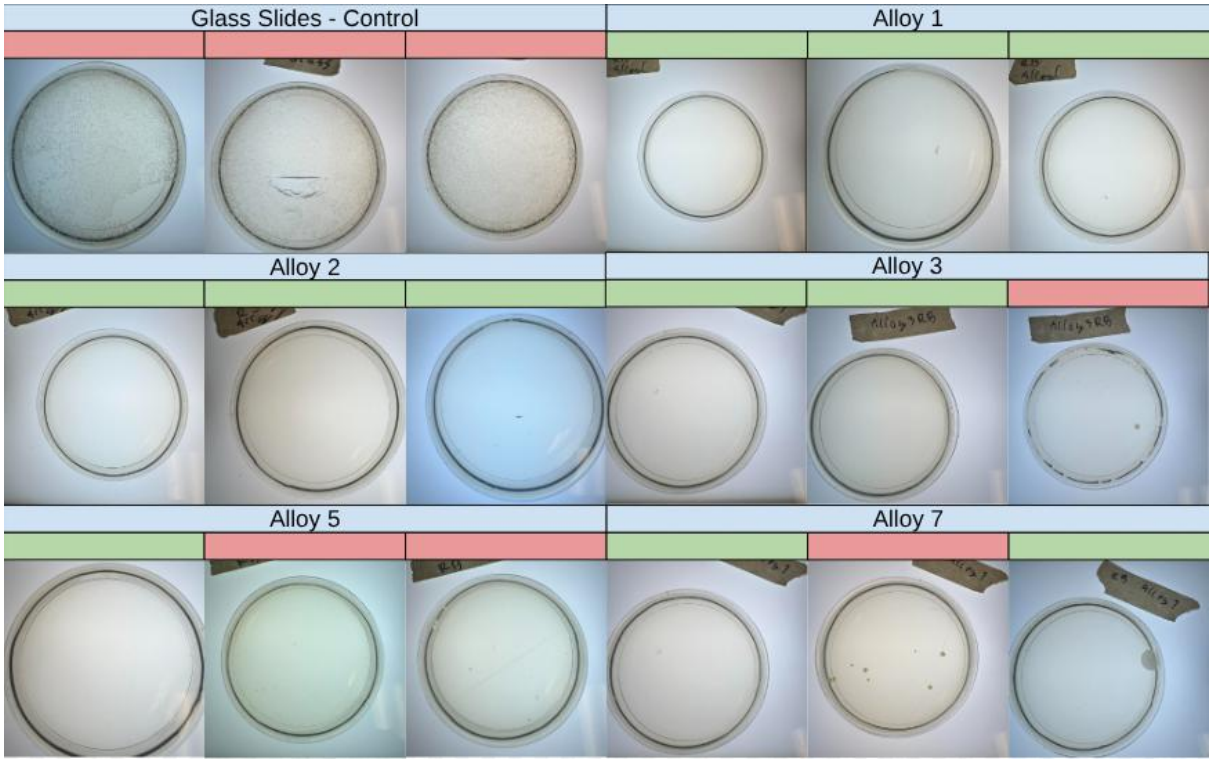

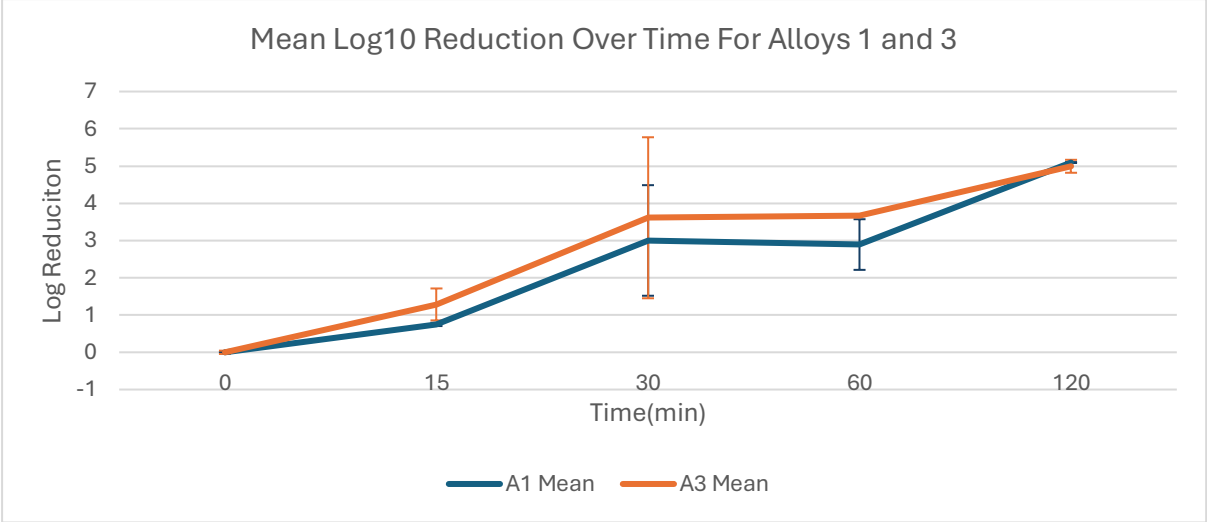

Figure 6-7: Antimicrobial Efficacy and Kinetic Kill Analysis. Top (Antimicrobial Assay): Visual comparison of bacterial growth across replicates for glass slide controls (red bars) and Alloys 1, 2, 3, 5, and 7 (predominantly green bars), where the absence of colonies in alloy-treated plates demonstrates widespread antimicrobial inhibition. Bottom (Log Reduction Kinetics): Mean log 10 reduction of bacterial load over a 120-minute period for Alloys 1 and 3, showing both materials achieving a significant 5-log reduction by the final time point. Note: Error bars represent standard deviation; green indicators denote successful antimicrobial replicates, while red indicates surviving bacterial presence.Alloy Series (1, 2, 3, 5, 7): Predominantly clear plates across various replicates, suggesting effective antimicrobial properties.). (Source: Student-generated data, 2025-26)

Alloys 4 and 8 were excluded from antimicrobial assaying due to the difficulty of cutting samples that could be used, because of their brittleness. Note that all alloys had film residue which could not be captured on camera.

All tested alloys showed signs of significant antimicrobial activity. Alloy activity is marked qualitatively: green indicates no visible colonies could be captured by camera, while red indicates viable colonies were observed. Alloy 5 had two plates with viable colonies, which was the most tested alloy. Alloy 7 had contamination seen in the bottom right plate, but no colonies observed.

These results were obtained using an experimentally determined 3.5×10^7 CFU count when counting a 4th dilution that was plated. If films are determined as non-CFU, it can be concluded that Alloys 1, 2, 3, and 7 achieved a maximum log reduction of ~5 within the two hours of contact.

Alloys 1 and 3 were tested further at additional time intervals. Log reduction of ~5 was achieved for both alloys in 2 hours, surpassing the EPA antimicrobial standard.

Statistical Note: In the log-reduction time-course study, only the 15-minute interval showed a statistically significant difference ($p < 0.05$) between the tested alloys.

SEM BSED Analysis and XRD Analysis

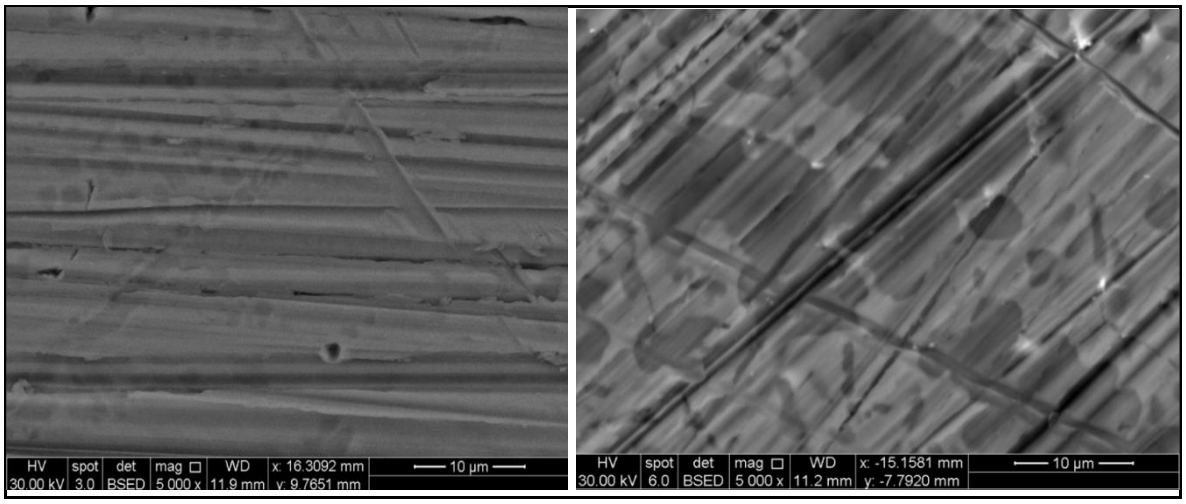

Figure 8-9-10: Backscattered Electron (BSE) Imaging: SEM/EDS analysis utilizing the backscattered electron technique provides elemental contrast across the surfaces of Alloys 5, 7, and 8, highlighting topographical features and material density variations at 10 um. Clockwise from top left is alloy 7,8 5.

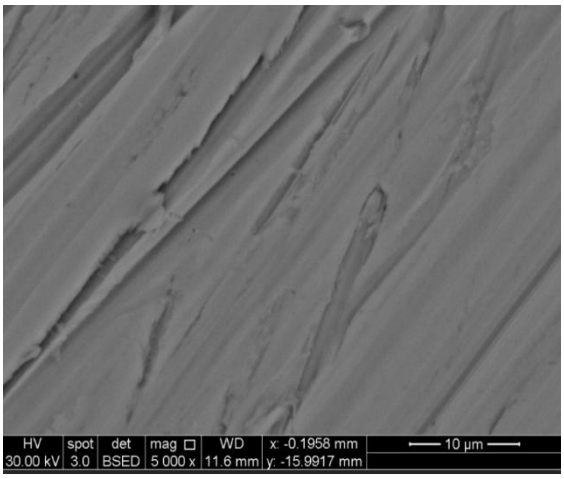

The BSED images of Alloys 5, 7, and 8 were spots chosen at random within the alloy samples.

Alloy 7 shows very small dark spots which indicate aluminum precipitates and potentially a grain boundary from the bottom left to the top right. Aside from the aluminum precipitates, there is consistent color across the image indicating homogeneous elemental distribution. Aluminum precipitates in the alloy could be the reason for the relative middle OCP compared to the other alloys. There was still aluminum present, but there was not too much uneven distribution, which would have caused aluminum to represent the dominant activity. The BSED scan also suggests this homogeneity, given the close weight percentages compared to the XRF data.

Alloy 8 shows major aluminum and impurity precipitates. The image sample also has elemental composition with major differences in its weight percentage composition when analyzed with BSED compared to XRF data. These elemental differences suggest that during casting, there was significant segregation of heavy and lighter elements. This heterogeneous structure of the alloy may also explain the poor corrosion resistance seen in the electrochemical data, as the microstructure could have corrosion weak spots since the elemental distribution was not uniform.

Alloy 5's homogeneous BSED image can be used to explain why the OCP was one of the more noble alloys studied. The consistent coloring and similar elemental composition received from BSED and XRF indicate a very homogeneous structure. This homogeneity allowed it to not be as reactive in a less corrosive environment than the impedance test, which is a harsher environment, and allowed it to undergo decline.

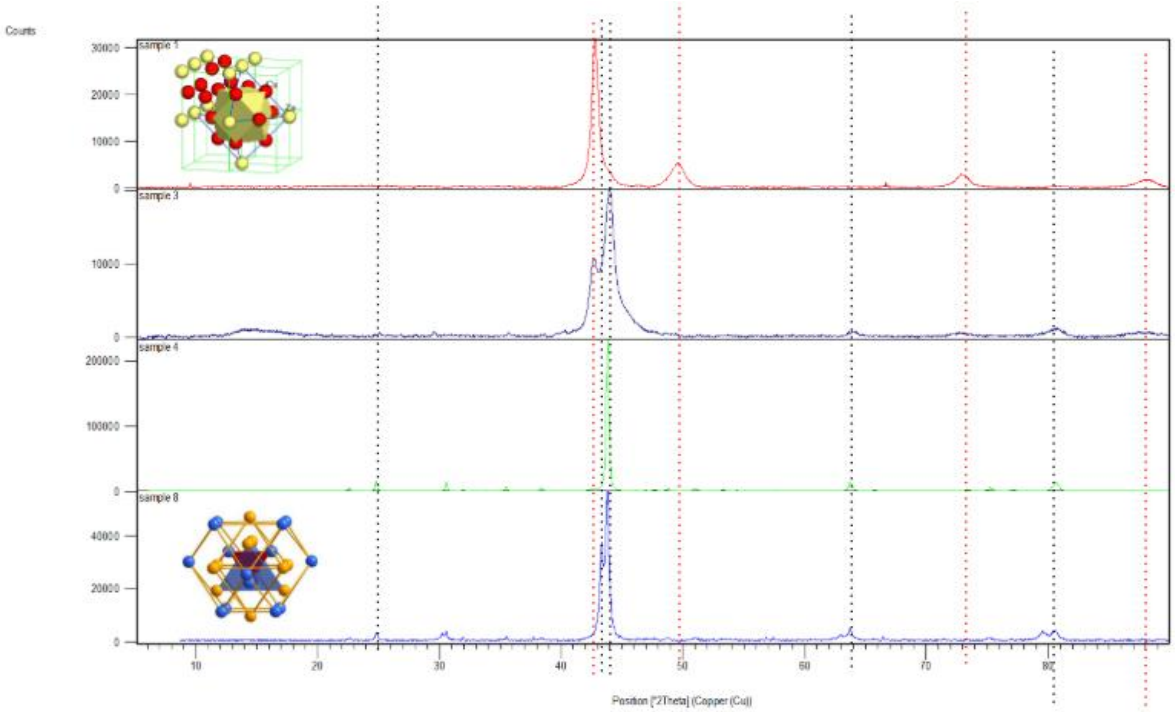

Figure 11: XRD Results with graphical additions of crystal structure of α and γ brass and line indicating potential crystalline structures.

Conclusions

Observed Trends

The ratio of zinc to aluminum was an important factor in determining corrosion resistance. A high ratio of zinc to aluminum appears to be the target when focusing on the corrosion aspect of an alloy. It should be taken into consideration, however, not to have too low of a copper-to-zinc ratio, or else dezincification can induce more corrosion.

Copper content did play a role in determining antimicrobial activity, as at least during $t \approx 15$ minutes, Alloy 3 with higher copper content outperformed Alloy 1. Aluminum content is also a determining factor in porosity and mechanical properties, as Alloys 4, 6, and 8 had to be excluded from some tests due to an inability to properly prepare samples.

Winning Alloy Candidates

Alloys 1, 3, and 7 are the alloys that warrant further research into similar or identical compositions due to their antimicrobial efficacy and corrosion resistance. Together, they demonstrate resistance to corrosion and antimicrobial activity without imbalancing the effect of either property.

Alloy 1 presents the desirable properties of both other candidate alloys but at a much lower copper content (approximately 69% Cu vs. 80%+ for Alloys 3 and 7). This makes Alloy 1 the best candidate tested for commercializing the alloy for antimicrobial use, as lower copper content reduces material cost—an important factor when weighing the benefits of implementation against the necessary resources required.

Future applications for Alloy 1 include powdered alloy paint for hospital settings (using latex paint base), handles, and tools. For marine applications, Alloy 3 may be more suitable due to its nobler electrochemical behavior, potentially limiting dezincification in seawater environments (using oil alkyd paint base).

Works Cited

David, R. (2011, December 16). Why zinc is bad for bacteria.*Nature News*. https://www.nature.com/articles/nrmicro2726

Foster, L. (2014).*Tarnishing of a Cu-Al-Zn-Sn alloy compared to commercially pure copper: Implications toward antimicrobial function*. (Doctoral dissertation, University of Virginia). LibraETD. https://libraetd.lib.virginia.edu/public_view/x633f118z

Horton, D. J., Ha, H., Foster, L. L., Bindig, H. J., & Scully, J. R. (2015). Tarnishing and Cu ion release in selected copper-base alloys: Implications towards antimicrobial functionality.*Electrochimica Acta*, 179, 352-366. https://doi.org/10.1016/j.electacta.2015.02.178

Khan, A., Mir, M. S., Hamid, R., & Wani, R. U. H. (2022). Antimicrobial copper-alloy touch surfaces: A game changer in ICUs.*Aditum Journal of Clinical and Biomedical Research*, 4(4). https://doi.org/07.2022/1.1082

Šulčius, A. (2010). Electrochemical properties of aluminum and its alloys in chloride solutions.*Materials Science*, 16(2), 110-116.

Tiryakioğlu, M. (2012). The effect of hydrogen on pore formation in aluminum alloy castings: Myth versus reality.*International Journal of Metalcasting*, 6(3), 7-15.

Zobac, O., et al. Phase equilibria in the Cu-Zn-Al system.*Journal of Alloys and Compound.*